

# Supporting Information for:

## Resolving the Structural Debate for the Hydrated Excess Proton in Water

Paul B. Calio,<sup>†</sup> Chenghan Li,<sup>†</sup> and Gregory A. Voth

Department of Chemistry, Chicago Center for Theoretical Chemistry, James Franck Institute, and Institute for Biophysical Dynamics, The University of Chicago, 5735 South Ellis Avenue, Chicago, Illinois 60637, United States

<sup>†</sup>These authors contributed equally to this work

### S1. Methodology and Accuracy Evaluation of EDS-BLYP-D3(OH)

The EDS(OH) correction was originally developed for the AIMD simulation of water.<sup>1</sup> When simulating water, the EDS(OH) potential (eq 3 in the main text) is turned off between O-H pairs within 1.2 Å to exclude bonded O-H atoms. A quantitative description on covalence is needed to apply the EDS(OH) potential to the excess proton in water and to smoothly switch on and off the bias during bond breaking and forming in the Grotthuss shuttle mechanism. Hence, a constrained density functional theory (CDFT) calculation at the  $\omega$ B97X/TZVP level was carried out in ref<sup>2</sup> to expand the ground-state wavefunction in the representation of diabatic states,  $|\psi\rangle = c_1|1\rangle + c_2|2\rangle$  (Figure S1). The charge transfer factor  $c_1^2/c_2^2$  between two diabatic states was then fitted to an exponential function of  $\delta$  (eq 7 in supplemental ref<sup>3</sup>) and the same procedure in refs<sup>2-3</sup> was followed to compute an approximate  $\mathbf{c}$  for the excess proton in liquid water. The EDS(OH) correction was computed in each diabatic state  $|i\rangle$  excluding bonded O-H pairs, and the final EDS force was a weighted average of the state-dependent EDS bias force,  $\mathbf{F}^{\text{EDS}} = \sum_i c_i^2 \mathbf{F}_i^{\text{EDS}}$ .

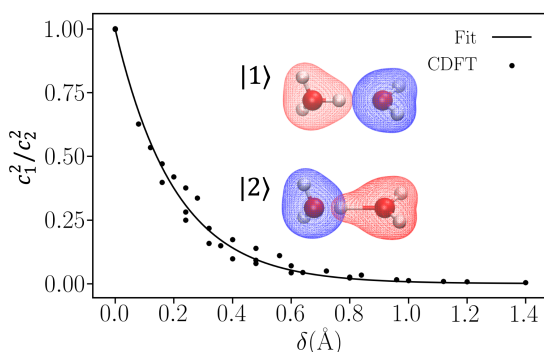


**Figure S1.** The charge transfer factor  $c_1^2/c_2^2$  from CDFT calculations and its exponential fit. The molecular figures show the definition of two diabatic states of  $\text{H}_5\text{O}_2^+$  defined in CDFT calculations.

The accuracy of the EDS(OH) correction to BLYP-D3 was first benchmarked for the proton transfer process in the gas-phase  $\text{H}_5\text{O}_2^+$  Zundel cation (Figure S2). As well as being a computationally efficient correction for the AIMD, the EDS (OH) also improves the BLYP-D3

functional significantly for the gas phase Zundel PT barrier and brings its accuracy to be comparable with the much more expensive hybrid function revPBE0-D3 as well as coupled cluster theory. It is also worth noting that the EDS correction was parametrized to correct hydrogen bonds in condensed-phase BLYP-D3 water, but it clearly is transferable to the gas-phase protonated water dimer PT process as is shown here.

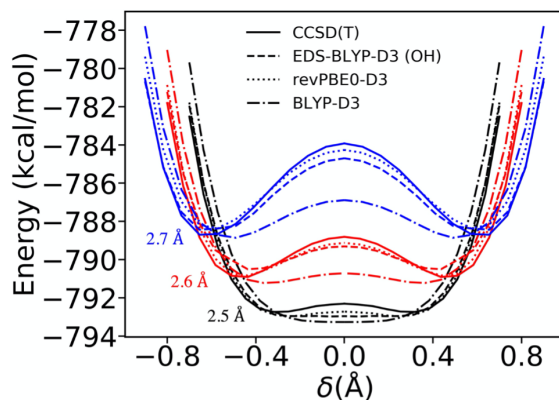


**Figure S2.** Potential energy surfaces of proton transfer in gas-phase  $\text{H}_5\text{O}_2^+$  from various computational methods.

The EDS-BLYP-D3(OH) was then benchmarked in the condensed phase system consisting of 1  $\text{H}^+$  in 128 waters. The diffusion constants of  $\text{H}^+$  and water are summarized in Table S1.

**Table S1: Diffusion constants in EDS-BLYP-D3(OH)**

	$D_{\text{H}_2\text{O}}$ ( $\text{\AA}^2/\text{ps}$ )	$D_{\text{H}^+}$ ( $\text{\AA}^2/\text{ps}$ )	$D_{\text{H}^+}/D_{\text{H}_2\text{O}}$	Ave. Temp(K)
EDS-BLYP-D3(OH)	$0.15 \pm 0.01$	$0.73 \pm 0.13$	$4.9 \pm 0.7$	$295 \pm 2.7$
Experiment	$0.23^a$	$0.94^b$	4.1	

<sup>a</sup> Taken from ref<sup>4</sup>

<sup>b</sup> Taken from ref<sup>5</sup>

## S2. RDFs of MS-EVB 3.2, aMS-EVB 3.2 and EDS-AIMD(OO)

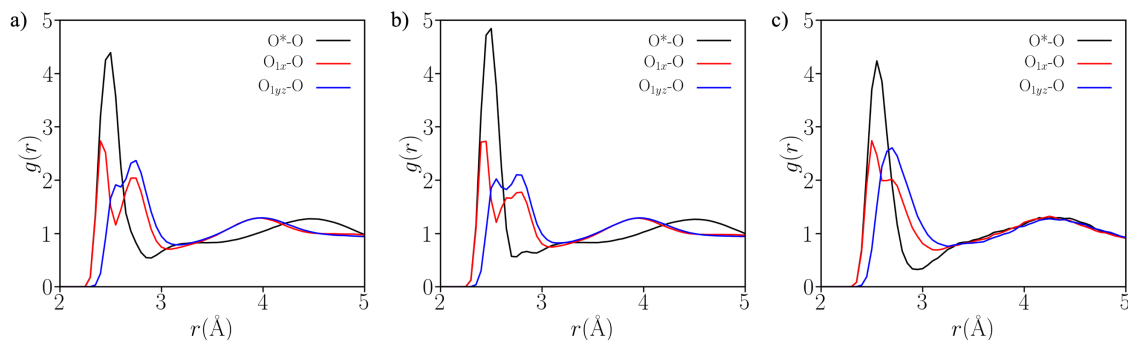


**Figure S3.** O-O radial distribution functions of the  $\text{O}^*\text{-O}$  (black),  $\text{O}_{1x}\text{-O}$  (red), and  $\text{O}_{1yz}\text{-O}$  (blue) in classical simulations of (a) MS-EVB, (b) aMS-EVB, and (c) EDS-AIMD(OO).

### S3. Classification of Eigen and Zundel Cations

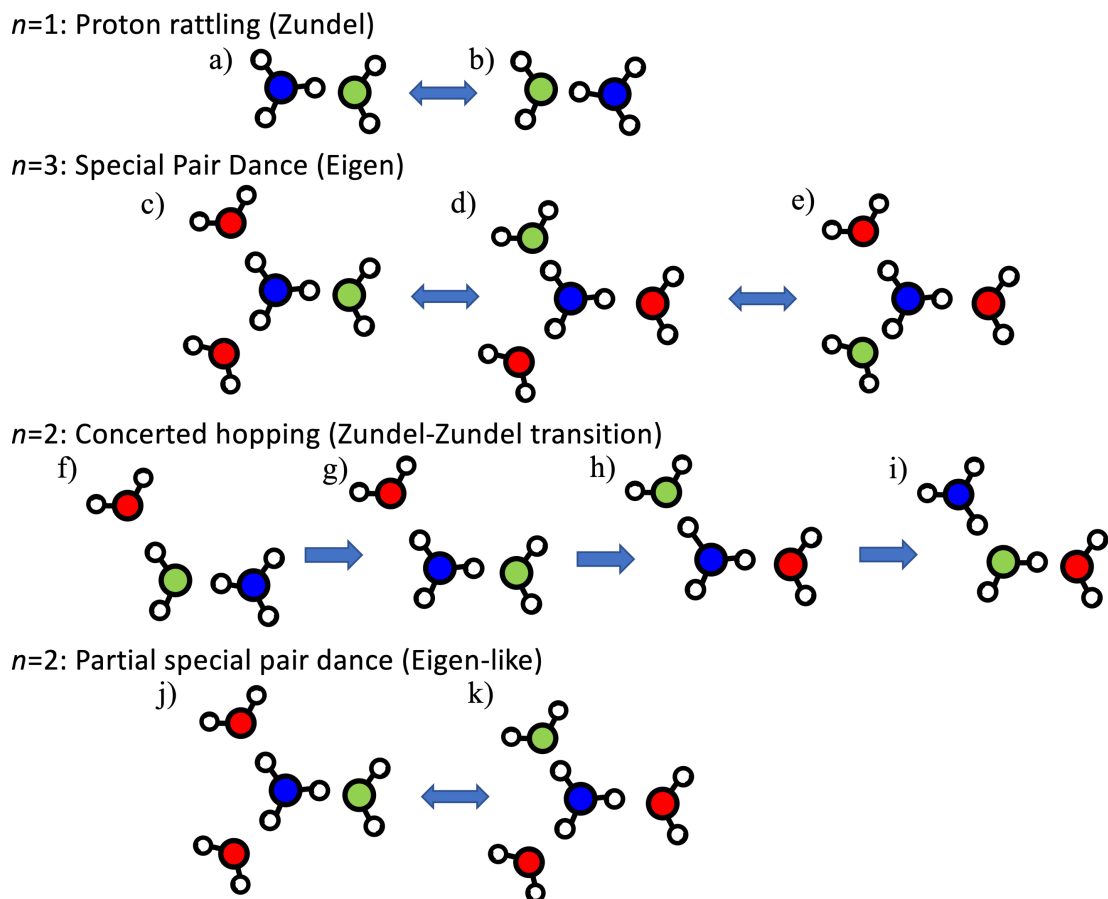


**Figure S4.** Illustration of the classification of Eigen and Zundel cations based on the number of unique special pairs ( $n$ ). The most probable hydronium is rendered in blue and the special pair partner is rendered in green.

The trajectory was first split into time segments where hopping events do not occur, i.e., the trajectory was partitioned into segments based on timesteps where the most hydronium-like oxygen identity was about to change. Within each segment, the number of unique special partners  $O_{1x}$  visited ( $n$ ) was counted, and the segments were consequently grouped together according to their  $n$  value. The total time length of each group was determined by summing the length of each segment in the group. The population of each group was defined as the group total time length over the length of the full trajectory.

In a proton “rattling” process, only one  $O_{1x}$  can be identified in the no-hopping period (Figure S4a,b), and the corresponding  $n$  value will be unity to indicate a Zundel cation. In the special pair dance, the  $O_{1x}$  visits three distinct coordinated waters of the central hydronium, and hence has an  $n$  value of three to indicate an Eigen cation (Figure S4c,d,e). An  $n$  value of 2 can be broken into two situations: (1) an intermediate state (Figure S4g,h) as part of a three-water concerted hopping process (Figure S4f,g,h,i), and (2) a partial special pair dance in which the third special partner is not visited yet before the proton hops (Figure S4j,k). These two,  $n = 2$  dynamics can be determined by verifying if the  $O_{1x}$  identity returns to a previous  $O_{1x}$  water in the same no-hopping period. If this is the case, then  $O_{1x}$  is resonating between two waters, and this indicates a partial

special pair dance segment. If  $O_{1x}$  visits two waters in a sequential manner, then this segment describes a concerted proton hopping process. We regard the concerted proton hopping better resembles the Zundel-Zundel transition mechanism and thus assign it to be Zundel. The partial special pair dance that features the  $O_{1x}$  resonating between two waters contributes to the spectroscopic anisotropy decay in a similar way as a complete special pair dance, and is thus assigned as Eigen. The resultant Eigen/Zundel population based on these assignments is shown in the Figure 1c inset, while the total population of each  $n$ -segment is shown in Figure S5 below.

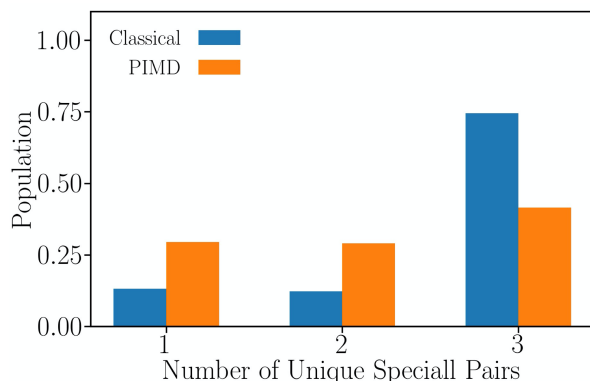


**Figure S5.** Population of trajectory segments as a function of  $n$  in classical and quantum EDS-BLYP-D3(OH) AIMD simulations.

#### S4. Anisotropy Decay Plots for MS-EVB 3.2 on a Log Scale

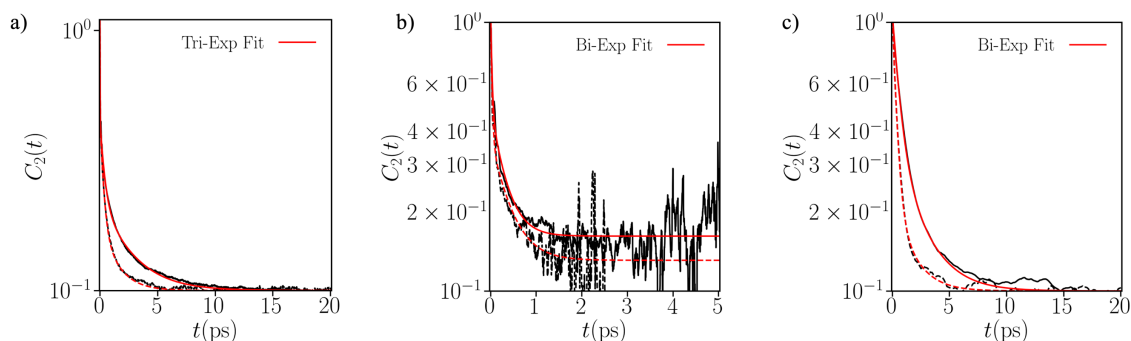


**Figure S6.** Anisotropy plots in log scale. The anisotropy plots are broken down based on (a) total anisotropy, (b) special pair dance (no proton transfer), and (c) long-lived special pair (no special pair dance). The solid curves represent the classical MS-EVB results while the dashed represent the quantum MS-EVB results. All the data was shifted by 0.1 to avoid the singularity of the log function at zero.

## S5. Anisotropy Decays for aMS-EVB 3.2, and EDS-AIMD

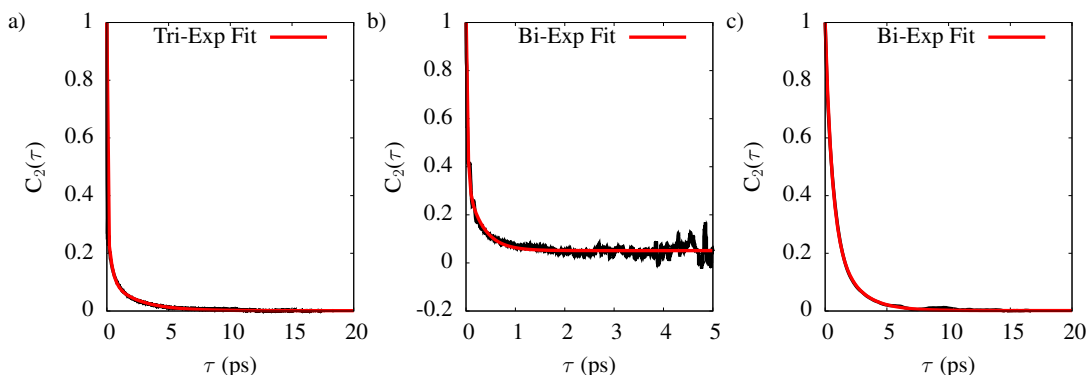


**Figure S7.** Anisotropy plots for the O<sup>\*</sup>-O<sub>w</sub> unit vector in aMS-EVB 3.2. The anisotropy plots are broken down based on (a) total anisotropy, (b) special-pair dance, and (c) long-lived special-pair.

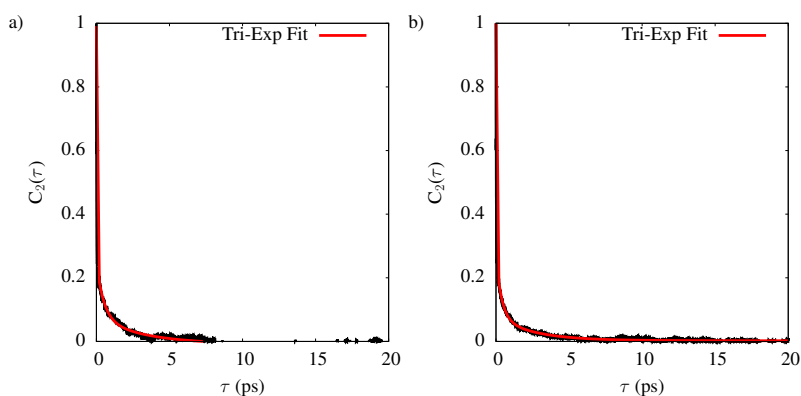


**Figure S8.** Total anisotropy plots for the O<sup>\*</sup>-O<sub>w</sub> unit vector in (a) EDS-AIMD(OO) and (b) EDS-AIMD(OH). Limited statistics prevent us from calculating the EDS-AIMD anisotropy of special-pair dance and long-lived special-pair.

## S6. Justification for Anisotropy Fitting Method

$$f(x) = a_1 \cdot \exp(-x/\tau_1) + a_2 \cdot \exp(-x/\tau_2) + a_3 \cdot \exp(-x/\tau_3) + C \quad S1$$

$$\text{where in the fitting procedure, } a_3 = (1 - a_1 - a_2)$$

### Total Anisotropy

Experimental anisotropy curves with fit using a bi-exponential fit. However, we found using tri-exponential fits best fit the curve as going from bi-exponential (Table S2) to tri-exponential (Table S3) increase the R<sup>2</sup> value on average increases by 0.01.

**Table S2: Bi-exponential Fit for Total Anisotropy**

System	$a_1$	$\tau_1$ (fs)	$a_2$	$\tau_2$ (ps)	C	$R^2$
MS-EVB	0.742	17.5	0.258	1.143	0.005	0.988
aMS-EVB	0.751	14.2	0.249	1.021	0.004	0.986
EDS-AIMD(OO)	0.806	21.5	0.194	1.402	-0.005	0.975
EDS-AIMD(OH)	0.807	21.6	0.193	1.048	0.0054	0.983

**Table S3: Tri-exponential Fit for Total Anisotropy**

System	$a_1$	$\tau_1$ (fs)	$a_2$	$\tau_2$ (ps)	$a_3$	$\tau_3$ (ps)	C	$R^2$
MS-EVB	0.649	12.3	0.234	0.363	0.117	2.472	0.001	0.998
aMS-EVB	0.661	10.1	0.229	0.324	0.110	2.267	0.001	0.997
EDS-AIMD(OO)	0.742	17.4	0.172	0.488	0.085	3.194	-0.009	0.984
EDS-AIMD(OH)	0.736	17.2	0.188	0.377	0.076	2.572	0.002	0.992

For a comparison to experimentally determined anisotropy timescales, the experimental data<sup>6</sup> at concentrations of 1M, 2M and 4M HCl were extrapolated to the 0.22 M for the MS-EVB simulations and 0.43 M for the EDS-AIMD simulations via a linear fitting (Figure S6).

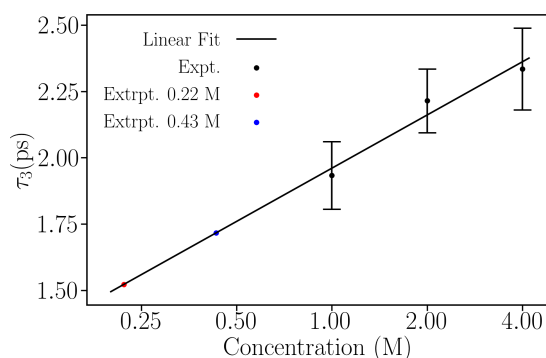


**Figure S9.** Extrapolation of experimental anisotropy timescale (referred as “slow component” in ref<sup>6</sup>) to the simulation concentrations. The extrapolated values are 1.5 ps for 0.22 M (red) and 1.7 ps for 0.43 M (blue). Note that the x-axis is plotted in log scale.

### Special-Pair Dance (No Hopping)

We fit the special-pair dance data to a bi-exponential curve as we expect the long-time, proton transfer process to be disregarded. When going from bi-exponential (Table S4) to tri-exponential (Table S5), the  $R^2$  value on average increases by 0.001. Additionally, MS-EVB can be an approximate bi-exponential fit since the third time constants is 0.0, and aMS-EVB does not have any time constants longer than 1 ps, meaning the long-time scale is essentially removed from the anisotropy decay.

**Table S4: Bi-exponential Fit for Special-Pair Dance**

System	$a_1$	$\tau_1$ (fs)	$a_2$	$\tau_2$ (ps)	C	$R^2$
MS-EVB	0.681	28.1	0.319	0.287	0.059	0.934
aMS-EVB	0.703	28.6	0.297	0.313	0.051	0.964

**Table S5: Tri-exponential Fit for Special-Pair Dance**

System	$a_1$	$\tau_1$ (fs)	$a_2$	$\tau_2$ (ps)	$a_3$	$\tau_3$ (ps)	C	$R^2$
MS-EVB	0.642	34.5	0.289	0.311	0.069	0.000	0.059	0.934
aMS-EVB	0.437	15.4	0.409	0.091	0.154	0.516	0.049	0.967

**Long-Lived Special Pair, No “Dance”**

We fit the long-lived, special-pair data to a bi-exponential curve as we expect the short-time, special-pair dance to be disregarded. When going from bi-exponential (Table S6) to tri-exponential (Table S7), the  $R^2$  value either remained constant or decreased when going from the bi-exponential fit to the tri-exponential fit. This seems to suggest that a bi-exponential fit can capture the proper physics of the system. Additionally, MS-EVB is essential a bi-exponential fit since the first time constant is close to zero.

**Table S6: Bi-exponential Fit for Long-Lived Special-Pair**

System	$a_1$	$\tau_1$ (ps)	$a_2$	$\tau_2$ (ps)	C	$R^2$
MS-EVB	0.737	0.557	0.263	2.169	0.003	0.907
aMS-EVB	0.672	0.533	0.328	1.795	0.002	0.902

**Table S7: Tri-exponential Fit for Long-Lived Special-Pair**

System	$a_1$	$\tau_1$ (fs)	$a_2$	$\tau_2$ (ps)	$a_3$	$\tau_3$	C	$R^2$
MS-EVB	0.052	0.4	0.786	0.682	0.162	2.889	0.001	0.907
aMS-EVB	0.043	4.0	0.885	0.955	0.072	0.001	0.006	0.900

**S7. Anisotropy Timescales of Pure Water**

The anisotropy decays of the water model SPC/Fw used in MS-EVB simulations were examined as well (Table S8). The anisotropy data was collected from 10 independent 1-ns-long NVE simulations of 256 water in a  $15.64 \times 15.64 \times 15.64 \text{ \AA}^3$  box. Two flavors of anisotropy calculations were performed: (1) the O-H bond unit vector was used in eq 5; (2) the hydrogen bond acceptor oxygen was resolved for every water, and the unit vector pointing from the water oxygen to its hydrogen bond acceptor oxygen was used in eq 5.

**Table S8: Bi-exponential Fit for SPC/Fw Water Anisotropy**

Anisotropy of	$a_1$	$\tau_1$ (ps)	$a_2$	$\tau_2$ (ps)	C	$R^2$
O-H Bond	0.32	0.13	0.68	2.68	0.00	0.9996
H-Bond Donor and Acceptor O-O	0.38	0.20	0.62	1.77	0.01	0.9988

## S8. Normal Mode Analysis Using Second Solvation Shell

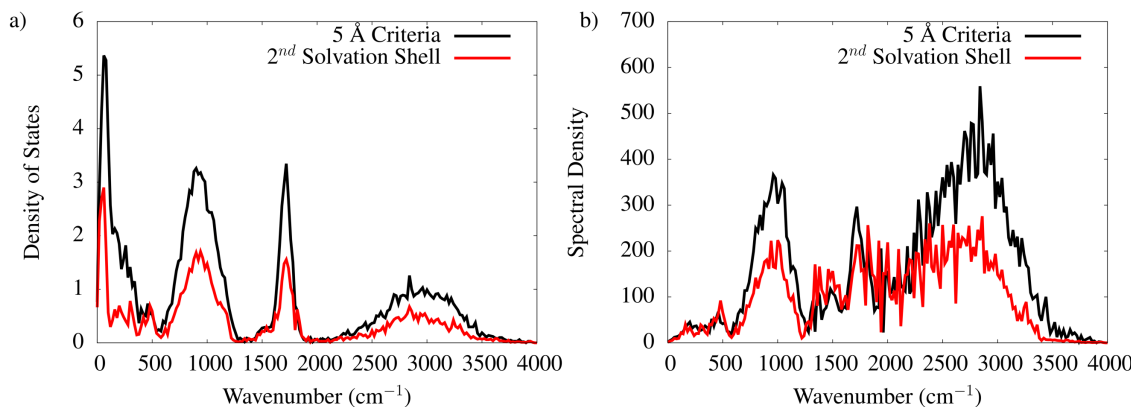


**Figure S10.** Density of States (a) and spectral density (b) from the INM analysis using the 5 Å cutoff and 2<sup>nd</sup> solvation shell cutoff. We observe that the only difference between the two radial cutoff methods is the intensity of the spectra.

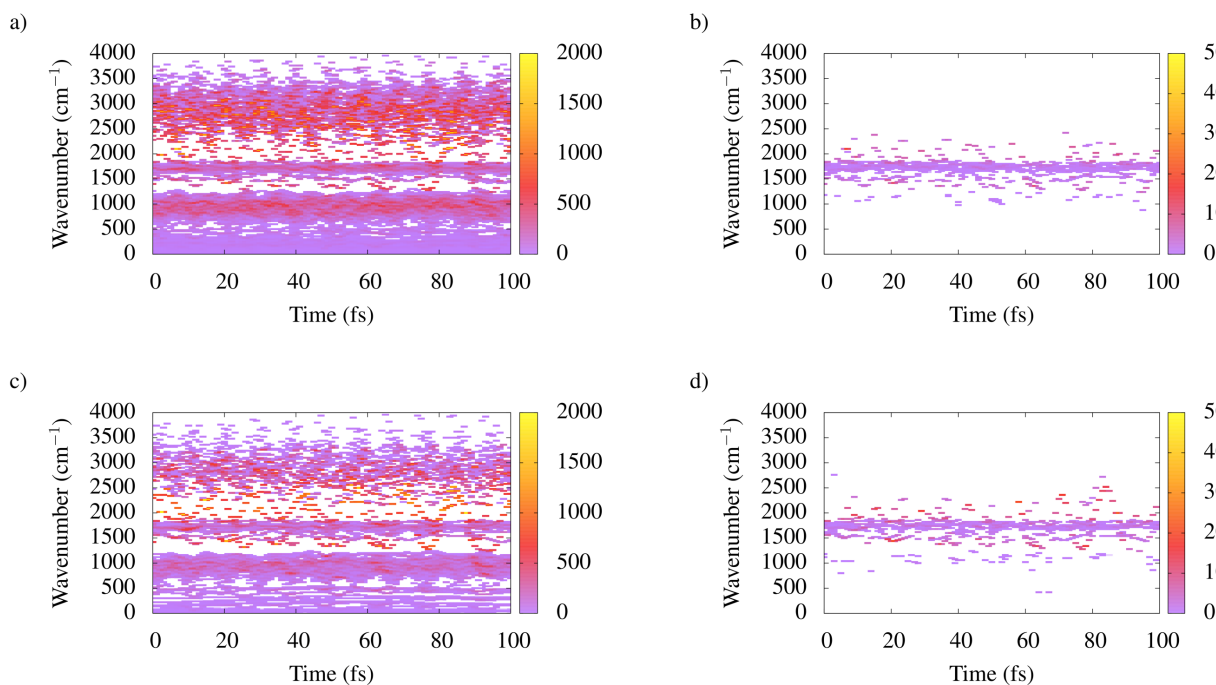


**Figure S11.** Spectral Density as a function of time for Eigen trajectories taken from MS-EVB 3.2 using the 5 Å cutoff (a & b) and 2<sup>nd</sup> solvation shell (c & d). Eigen trajectory is defined based on have 3 unique special-pair water molecules during the 100 fs segment. In Fig. (a) and (c) we show the total spectral density, while in Fig (b) and (d) we show the spectral density for H-O-H bends >5° in the special-pair. The same spectroscopic features corresponding to flanking water bending is independent of the radial cutoff method.

## S9. Spectral Density of Flanking Water Bend on EDS-AIMD Trajectories

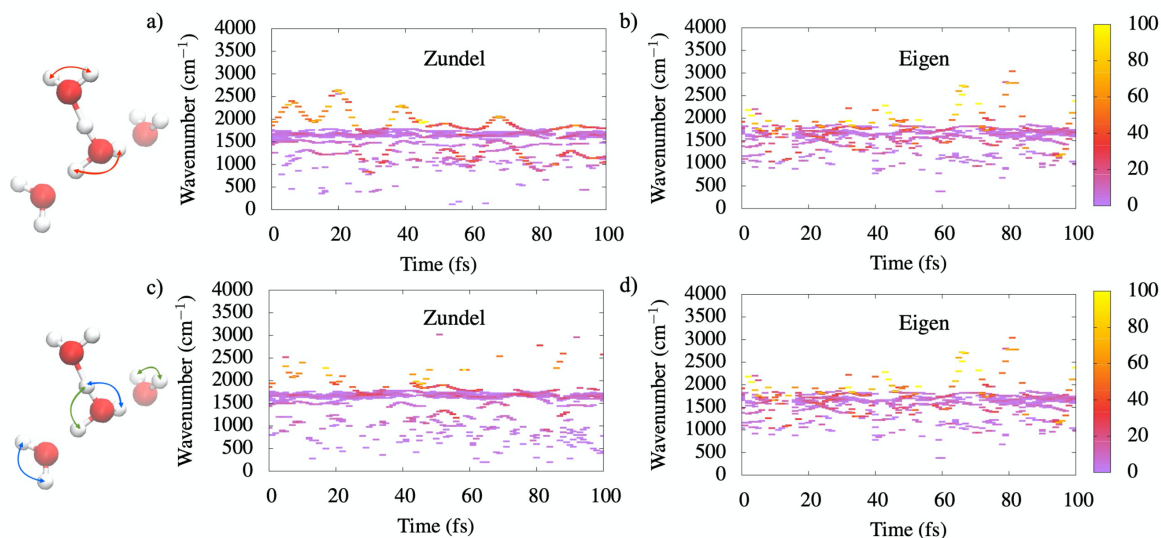


**Figure S12.** Spectral density as a function of time for H-O-H bends in a Zundel (a & c) period and an Eigen (b & d) period using data obtained from EDS(OO) simulations. Panels a and b show the spectral density for H-O-H bends >5° in the special pair, while Panels c and d show the spectral density of H-O-H bends >5° in other O\*-O pairs.

## Supplemental References

1. Calio, P. B.; G. M. Hocky; G. A. Voth, Minimal Experimental Bias on the Hydrogen Bond Greatly Improves Ab Initio Molecular Dynamics Simulations of Water. *J. Chem. Theory Comput.* **2020**, *16*, 5675-5684.
2. Li, C.; G. A. Voth, Using Constrained Density Functional Theory to Track Proton Transfers and to Sample Their Associated Free Energy Surface. *J. Chem. Theory Comput.* **2021**, *17*, 5759-5765.
3. Li, C.; J. M. J. Swanson, Understanding and Tracking the Excess Proton in Ab Initio Simulations; Insights from IR Spectra. *J. Phys. Chem. B* **2020**, *124*, 5696-5708.
4. Krynicky, K.; C. D. Green; D. W. Sawyer, Pressure and Temperature-Dependence of Self-Diffusion in Water. *Faraday Discuss* **1978**, *66*, 199-208.
5. Roberts, N. K.; H. L. Northey, Proton and Deuteron Mobility in Normal and Heavy-Water Solutions of Electrolytes. *J Chem Soc Farad T 1* **1974**, *70*, 253-262.
6. Carpenter, W. B.; N. H. C. Lewis; J. A. Fournier; A. Tokmakoff, Entropic barriers in the kinetics of aqueous proton transfer. *J. Chem. Phys.* **2019**, *151*, 034501.